JBUON 2021; 26(4): 1612-1622
ISSN: 1107-0625, online ISSN: 2241-6293 • www.jbuon.com
Email: editorial_office@jbuon.com

ORIGINAL ARTICLE

A nomogram concerning immune infiltration and radiosensitivity to predict biochemical recurrence after radical radiation therapy in prostate cancer

Chunyan Qiu[1], Xingni Zhou[2], Zhijian Chen[1], Hua Ren[1]

[1]National Cancer Center/National Clinical Research Center for Cancer, Cancer Hospital Chinese Academy of Medical Sciences, Shenzhen Center, Shenzhen 518116, China. [2]Department of Urology, Changhai Hospital, the Second Military Medical University, Shanghai 200433, China

Summary

Purpose: *To construct a nomogram concerning immune infiltration and radiosensitivity to predict biochemical recurrence (BCR) after radical radiation therapy in prostate cancer (PCa).*

Methods: *The Affymetrix microarray GSE116918 was acquired from the Gene Expression Omnibus (GEO) database. This cohort was grouped into biochemical recurrence ("BCR" group), among whom some patients developed metastatic recurrence ("MET" group), while the other patients were free from biochemical recurrence ("NO" group). Gene set enrichment analysis (GSEA) was performed. Immune infiltration was quantified by CIBERSORT, and infiltration score (IFS) and radiosensitivity score (RSS) were constructed. Cox multivariate regression coefficients were used to generate a nomogram.*

Results: *Compared to patients in the NO group, patients in the BCR group tended to be in a higher T stage (56.8% in T1-T2 vs 43.15% in T3-T4) (<0.05). IFS was calculated based on the infiltration level of neutrophils, macrophages, plasmacytoid dendritic cells (pDC), activated dendritic cells (aDC), and CD56 bright NK cells. Patients in the IFS-low group had a significantly longer BCR-free survival than those in the IFS-high group (p<0.0001). RSS was calculated based on the expression levels of BRCA2, IGF1, BCL2L1, MAPK1, MAPK6, and MAPK13. Patients in the RSS-low group had a significantly longer BCR-free survival than those in the RSS-high group (p<0.0001). A nomogram predicting BCR after radical radiation therapy in PCa showed a 95% CI of [0.6584, 0.7928] for C-index, an AUC of 0.741 at 5 years, and fine calibration.*

Conclusions: *In this study, we constructed a visual nomogram to predict BCR after radical radiation therapy in PCa with fine discriminatory and calibration capacity, which took elements, such as immune infiltration and radiosensitivity, into consideration for the first time.*

Key words: *nomogram, immune infiltration, radiosensitivity, prostate cancer*

Introduction

Prostate cancer (PCa) is the second most common cancer (after lung cancer) in men and the fifth leading cause of cancer death worldwide. It accounted for 1,276,106 new cases and caused 358,989 deaths (3.8% of all deaths caused by cancer in men) in 2018 [1]. Currently, radiotherapy plays an important role in the treatment of PCa. From a radiotherapy standpoint, low-risk localized PCa is treated by image guided intensity-modulated radiotherapy (IMRT) or brachytherapy provided the patients meet the required eligibility standards. Intermediate-risk patients may benefit from

Corresponding author: Hua Ren, MD. National Cancer Center/National Clinical Research Center for Cancer, Cancer Hospital Chinese Academy of Medical Sciences, Shenzhen Center, No. 113 Baohe Ave, Longgang District, Shenzhen 518116, China.
Tel: +86 13601168810, Fax: +86 0755 668676842, Email: hr1u1k@163.com
Received: 13/10/2020; Accepted: 02/12/2021

IMRT combined with 4–6 months of androgen deprivation therapy; IMRT alone or IMRT combined with brachytherapy can be administered to patients unsuitable for androgen deprivation treatment because of co-morbidities or unwillingness to take the treatment to maintain their sexual health. High-risk PCa, i.e. high-risk localized and locally advanced PCa, requires IMRT combined with long-term (≥2 years) androgen deprivation treatment with luteinizing hormone releasing hormone agonists [2].

However, biochemical recurrence (BCR) rates after primary radiation therapy (RT) for PCa have been reported to range between 22% and 69%, depending on different series [3]. BCR is characterized by elevated PSA after primary treatment, which usually precedes clinical recurrence and disease progression for many years [4]. Resistance to radiotherapy is primarily constituted by intrinsic factors such as cell radiosensitivity [5] as well as extrinsic factors such as tumor microenvironment (TME). It has been frequently reported that immune cell infiltration is associated with the effect of tumor radiation [6]. So far, there has been no systemic research on the involvement of cell radiosensitivity and immune infiltration in radiotherapy for PCa. Hence, we attempted to construct a nomogram concerning immune infiltration and radiosensitivity to predict BCR after radical radiation therapy in PCa.

Methods

Microarray data acquisition and data pre-processing

The Affymetrix microarray GSE116918 [7] taken in the platform of GPL25318 [ADXPCv1a520642] Almac Diagnostics Prostate Disease Specific Array (DSA) was acquired from the Gene Expression Omnibus (GEO, http://www.ncbi.nlm.nih.gov/geo/) database. GEO database is a high throughput biological database repository supported by the National Center for Biotechnology Information (NCBI) at the National Library of Medicine (NLM).

According to the description, this cohort contained 248 localized/locally advanced PCa patients commencing radical radiotherapy (with ADT). Patients were treated with 70-74 Gy external beam radiation therapy (EBRT) in 2 Gy fractions with 3D conformal or intensity modulated techniques over 7-7.5 weeks. Node-negative patients received elective pelvic nodal irradiation at the physician's discretion, and node-positive patients received radiotherapy to the pelvic nodal regions. A short (6 months) or long (>6–36 months) course of ADT was commenced at least 3 months before radiation with LHRH agonists or antiandrogens (https://www.ncbi.nlm.nih.gov/geo/query/acc.cgi?acc=GSE116918).

For handling 25 missing values of the T stage of tumor, multiple imputation by "mice" package in R was adopted, where poly-regression was fitted with Gleason score and age taken as independent variables.

Gene set enrichment analysis (GSEA)

The normalized expression profiles of free from biochemical recurrence (defined as "NO group") and BCR groups were analyzed via GSEA using the Broad Institute's GSEA software (http://www.broadinstitute.org/gsea). By evaluating expression data at the level of the whole gene set rather than just the statistically significant genes, GSEA reveals many biological pathways in common [8]. MSigDB gene sets (v.6.2) were referred, including Kyoto Encyclopedia of Genes and Genomes (KEGG) gene sets (c2.cp.kegg), Gene Ontology gene sets (C5.all), and immunologic signature gene sets (c7.all). Analyses were run with 1000 permutations of gene sets (size 15–1000) using the Signal2noise ranking metric.

Infiltration levels for immune cell type quantification

In recent years, it has been found that computational techniques applied to gene expression profiles of bulk tumors can rapidly provide a broader perspective on the intratumoral immune landscape [9]. An algorithm, CIBERSORT, was used to deconvolve the relative purity of 22 tumor-infiltrating immune cell subsets in samples with default parameters [10].

We employed the ssGSEA [11] implementation in R package "gsva" [12] to computationally assess the absolute infiltration levels of immune cell types. ssGSEA measures the per sample overexpression level of a particular gene list by comparing the ranks of the genes in the gene list with those of all other genes. Marker genes for 24 immune cell types (dendritic cells [DCs], immature DCs [iDCs], activated DCs [aDCs], plasmacytoid DCs [pDC], cytotoxic cells, neutrophils, eosinophils, mast cells, macrophages, natural killer cells [NKs], NK CD56dim cells, NK CD56bright cells, B cells, T cells, T helper cells, T helper 1 [Th1], T helper 2 [Th2], T helper 17 [Th17], T gamma delta [Tgd], CD8+ T, T central memory [Tcm], T effector memory [Tem], and T follicular helper [Tfh] cells and Treg cells) were obtained from the study by Bindea et al [9]. Normalized microarray datasets mentioned above were provided as input without further processing (i.e. no standardization or log transformation). A typical execution is gsva (data, list_of_signatures, method="ssgsea"). The output for each signature is a near-Gaussian list of decimals that can be used in visualization/statistical analysis without further processing.

Infiltration score (IFS) and radiosensitivity score (RSS) construction and grouping

It has been previously unraveled that several candidate genes with deletion or loss of function mutations may be associated with altered cellular radiosensitivity (e.g., ATM, p53, BRCA1, BRCA2, DNA-PK) [13]. Therefore, based on a vast review of literature, we chose HIF1A [14], NFKB1 [15], NFKB2, REL [16], RELA, RELB, BCL2 [17], APAF1 [18], CASP3 [19], PRKDC [20], ATM [21], TP53 [22], BRCA1 [23], BRCA2 [24], KRAS [25], NRAS [26], HRAS [27], MYC [26], RAF1 [28], ABL1 [29], MOS, IGF1 [30], BCL2L1 [31], IL1A, IL1B, TNF [32], MAPK1, MAPK6, MAPK4, MAPK3, MAPK9, MAPK8, MAPK7, MAPK14, MAPK15, MAPK12, MAPK13, MAPK10, and MAPK11 [33] as candidate radiosensitivity-related genes.

We used the LASSO Cox regression model for patients' BCR free survival through "glmnet'' package in R to select the most useful prognostic features out of all the absolute number of immune cell infiltration quantified by ssGSEA, and expression of radiosensitivity- related genes. Here, we included those with a metastasis event into groups with BCR event. We then derived formulas to calculate, the IFS and RSS for all patients based on their personalized level of selected features.

The optimum cutoff IFS and RSS scores were selected on the basis of the association with the patients' BCR free survival by using X-tile software version 3.6.1 (Yale University School of Medicine, New Haven, CT, USA). Therefore, we grouped the patients according to the cut-off point and defined the groups as the IFS-high/IFS-low and the RSS-high/RSS-low groups.

Development of a prognostic nomogram

We used the Cox regression model to perform the univariate and multivariate survival analysis. Cox multivariate regression coefficients were used to generate a nomogram. The concordance index (C-index) and receiver operating characteristic (ROC) curve were used to determine its discriminatory capacity. Calibration plots were generated to explore the calibration capacity of the nomogram. Nomogram and calibration plots were generated with the "rms" package of R software.

Statistics

Continuous variables were compared by the Student *t*-test and presented as mean ± standard deviation. Categorical variables were compared by the chi-square test, and presented in percentages. For survival analyses, we used the Kaplan-Meier method to analyze the correlation between variables and BCR free survival and the log-rank test to compare survival curves. All statistical tests were two tailed, where a p value <0.05 was considered statistically significant. Statistical analyses were performed using R version 3.1.2 (R Foundation for Statistical Computing, Vienna, Austria).

Results

Patients' baseline characteristics

The median follow-up time was 82 months. As shown in Table 1, a total of 248 localized/locally advanced PCa patients were included. Fifty-six patients developed biochemical recurrence ("BCR" group), among which 22 patients developed metastatic recurrence ("MET" group), while the other 192 patients were free from biochemical recurrence ("NO" group). The age of the whole cohort was 67.35 ± 6.36 years. Patients with T3 stage (41.54%) and Gleason score of 7 (39.92%) accounted for most of the patients. Compared to patients in the NO group, patients in the BCR group tended to be in a higher T stage (56.85% in T1-T2 vs. 43.15% in T3-T4) (p<0.05).

GSEA

Figure 1A and Figure 1B show the top 20 KEGG pathway/GO terms/immunologic signatures that the genes were enriched for in the NO and BCR groups, respectively. Although genes in these two groups were enriched in a wide variety of KEGG pathway/GO terms/immunologic signatures, not much specificity was observed in two groups.

Relative infiltration levels for immune cell types

We estimated the mean relative fractions of 22 types of immune cells by CIBERSORT. As demonstrated by cumulative bar graphs in Supplementary Figure 1, T cells CD8 (32.3, 31.6 and 34.8%), mast cells resting (16.1, 15.6 and 14.9%), macrophages M0 (8.3, 8.6 and 7.6%), T cells follicular helper (7.1, 5.6 and 6.3%), and B cells memory (6.9, 5.5 and 6.6%) presented the top five maximum mean fractions in the NO, BCR, and MET groups.

Table 1. Clinical characteristics

Variables	*Total (N=248)* *n (%) / Mean±SD*	*NO (N=192)* *n (%) / Mean±SD*	*BCR (N=56)* *n (%) / Mean±SD*	*p*⁺
Age (years)	67.35±6.36	67.71±6.04	66.13±7.28	0.1400*
T stage				0.0102
T1	59 (23.79)	51 (26.56)	8 (14.29)	
T2	82 (33.06)	66 (34.38)	16 (28.57)	
T3	103 (41.54)	74 (38.54)	29 (51.79)	
T4	4 (1.61)	1 (0.52)	3 (5.35)	
Gleason score				0.5645
6	42 (16.94)	36 (18.76)	6 (10.71)	
7	99 (39.92)	77 (40.10)	22 (39.29)	
8	52 (20.97)	39 (20.31)	13 (23.21)	
9	54 (21.77)	39 (20.31)	15 (26.79)	
10	1 (0.40)	1 (0.52)	0 (0)	

⁺The p value of the difference between groups is calculated by chi-square test when not specified. * The p value is calculated by t-test.

IFS construction and grouping

LASSO Cox regression model was used to build a prognostic classifier, which included the following five features out of the 24 infiltration features of the immune cell type identified in the whole cohort: neutrophils, macrophages, pDC, aDC, and NK_CD56bright (Figure 2A). We then derived a formula to calculate the IFS for all patients based on their personalized levels of the five features, where IFS=-0.34*infiltration level of neutrophils+7.55*infiltration level of macrophages+1.15* infiltration level of pDC+2.20*infiltration level of aDC+0.64* infiltration level of NK_CD56bright.

We then compared the absolute infiltration levels of immune cell types on ssGSEA among NO, BCR, and MET groups with ANOVA. The boxplot in Figure 2B illustrates that infiltration levels of macrophages ($p<0.01$), pDC ($p<0.01$), and aDC ($p<0.05$) in the BCR group were significantly higher than those in the NO group. The absolute infiltration levels of other immune cell types, including neutrophils and NK_CD56bright, did not show any significant differences among the three groups.Using X-tile plots, we classified the patients into IFS-high and IFS-low groups with an IFS cutoff value of 0.66. Distribution of age and T stage did not vary significantly between the IFS-high and IFS-low groups ($p>0.05$), however, patients with low

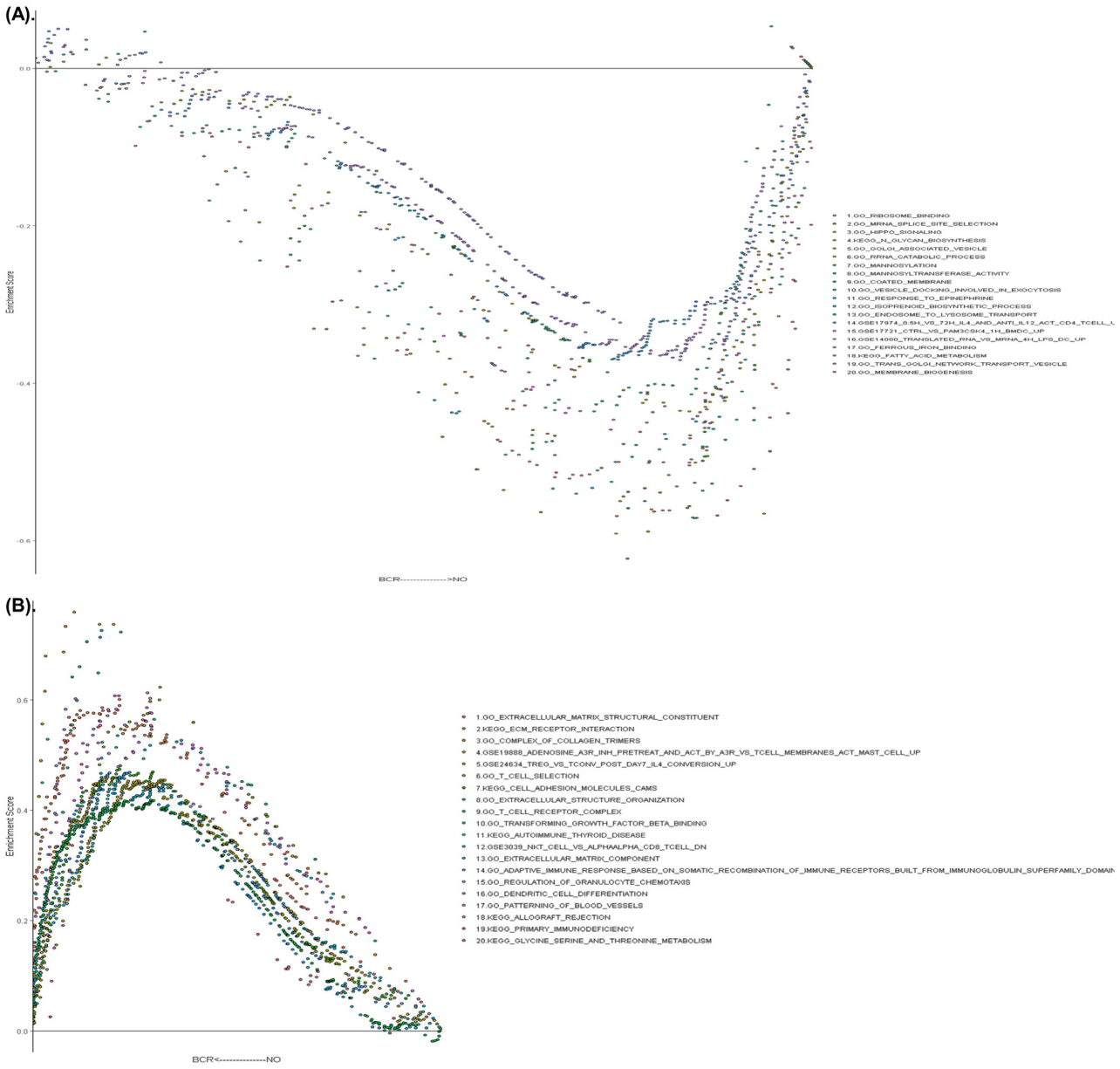

Figure 1. The top 20 KEGG pathway/GO terms/immunologic signatures enriched. **A:** Signatures enriched in NO group. **B:** Signatures enriched in BCR group.

IFS tended to have lower Gleason score than those with high IFS (60.42 vs. 44.64% with Gleason score of 6-7, p<0.05) (Table 2). As shown in Figure 2C, patients in the IFS-low group had a significantly longer BCR-free survival than those in the IFS-high group (p<0.0001). To eliminate the effect of Gleason score, we constructed the K-M plot of BCR-free survival in IFS groups adjusted for Gleason score, and it showed that this finding was not affected by Gleason score (Supplementary Figure 2).

RSS construction and grouping

As for the RSS, the following 6 genes out of the 39 radiosensitivity-related genes were selected by LASSO Cox regression model from the whole cohort: BRCA2, IGF1, BCL2L1, MAPK1, MAPK6, and MAPK13 (Figure 3A). The following formula was derived to calculate RSS for all patients based on their personalized expression levels of the 6 genes: RSS=0.33* expression level of BRCA2-0.27* expression level

Table 2. Clinical characteristics and IFS

Variables	*Total* *n (%)*	*IFS-low* *n (%)*	*IFS-high* *n (%)*	*p**
Age (years)				0.8598
≤68	131 (52.82)	102 (53.13)	29 (51.79)	
>68	117 (47.18)	90 (46.88)	27 (48.21)	
T stage				0.0734
T1/T2	141 (56.85)	115 (59.90)	26 (46.43)	
T3/T4	107 (43.15)	77 (40.10)	30 (53.57)	
Gleason score				0.0360
6-7	141 (56.85)	116 (60.42)	25 (44.64)	
8-10	107 (43.15)	76 (39.58)	31 (55.36)	

* The p value is calculated by chi-square test.

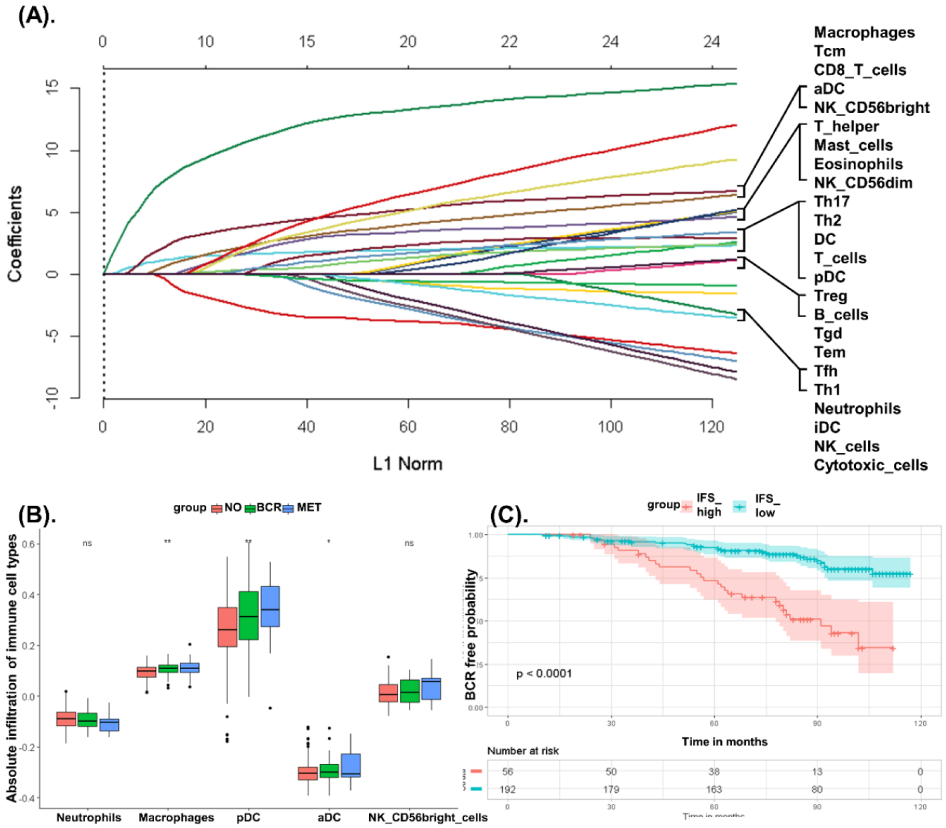

Figure 2. IFS construction and grouping. **A:** LASSO coefficient profiles of the 24 infiltration of immune cell type features. **B:** Absolute infiltration of 5 selected immune cell types in NO, BCR and MET groups. **C:** Kaplan-Meier BCR-free survival in the IFS_high and IFS_low groups.

of IGF1+0.28* expression level of BCL2L1-0.07* expression level of MAPK1-0.01* expression level of MAPK6+0.13* expression level of MAPK13.

We then compared the expression levels of these radiosensitivity- related genes among the NO, BCR, and MET groups with ANOVA. The boxplot in Figure 3B illustrates that the expression level of BCL2L1 in the BCR group was significantly higher than that in the NO group ($p<0.05$), while the expression level of IGF1 in the BCR group was significantly lower than that in the NO group ($p<0.01$). The expression levels of other genes, including BRCA2, MAPK1, MAPK6, and MAPK13 did not show any significant differences among the three groups.

Using X-tile plots, we classified the patients into RSS-high and RSS-low groups with an RSS cutoff value of 2.23. The two groups showed no significant difference in age distribution ($p>0.05$). Patients with low RSS tended to be in a lower T

Table 3. Clinical characteristics and IFS

Variables	*Total* *n (%)*	*RSS-low* *n (%)*	*RSS-high* *n (%)*	*p**
Age (years)				0.4561
≤68	131 (52.82)	92 (54.44)	39 (46.99)	
>68	117 (47.18)	77 (45.56)	40 (53.01)	
T stage				0.0142
T1/T2	141 (56.85)	105 (62.13)	36 (45.57)	
T3/T4	107 (43.15)	64 (37.87)	43 (54.43)	
Gleason score				0.0010
6-7	141 (56.85)	108 (63.91)	33 (41.77)	
8-10	107 (43.15)	61 (36.09)	46 (58.23)	

* The p value is calculated by chi-square test.

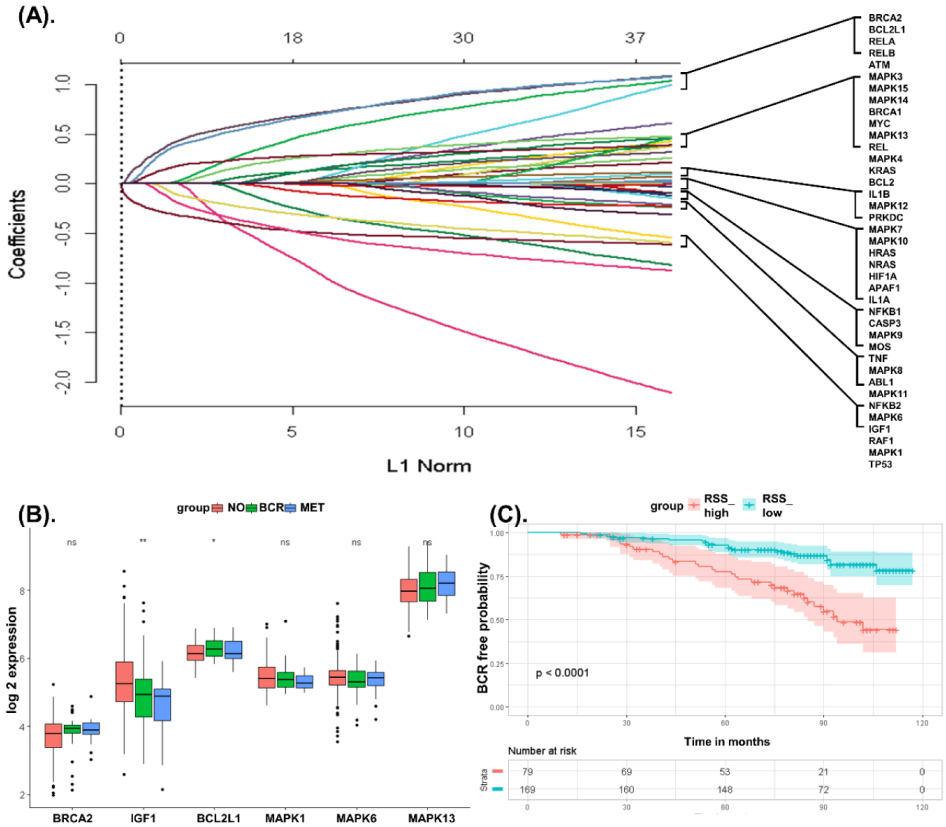

Figure 3. RSS construction and grouping. **A:** LASSO coefficient profiles of the 39 radiosensitivity related genes features. **B:** Log 2 expression of 6 selected genes in NO, BCR and MET groups. **C:** Kaplan-Meier BCR-free survival in the RSS_high and RSS_low groups.

stage and have a lower Gleason score than those with high RSS (62.13 vs. 45.57% in the T1/T2 stage, p<0.05; 63.91 vs. 41.77% in Gleason score of 6-7, p<0.05) (Table 3). As shown in Figure 3C, patients in the RSS-low group had a significantly longer BCR-free survival than those in the RSS-high group (p<0.0001). Supplementary Figure 3 and Figure 4 show that this finding was not affected by Gleason score or T stage.

Development of a prognostic nomogram

To provide a clinically relevant quantitative method to predict the 1-, 3-, and 5-year BCR-free probability in patients with PCa, we constructed a nomogram based on Cox multivariate regression that integrated the IFS group, RSS group, and clinicopathological risk factors (Figure 4A).

The larger the C-index, the more favorable the predictive accuracy of the model. It showed that this model had a 95% confidence interval of [0.6584, 0.7928] for C-index. Additionally, this model obtained a fine AUC of 0.741 at 5 years (Figure 4B). These two indexes showed that the model had great discriminatory capacity.

Calibration is useful for assessing whether actual outcomes resemble predicted outcomes for every nomogram. The x-axis represents the prediction calculated with use of the nomogram, and the y-axis represents the actual freedom from BCR in patients. The 45-degree line represents the performance of an ideal nomogram, in which the predicted outcome perfectly corresponds with the actual outcome. It showed that the nomograms performed well compared with the performance of an ideal model (Figure 4C).

Discussion

Although BCR of PCa generally precedes clinical progression, about one-third of men survive for 15 years after BCR, one-third die of PCa, and one-third die of competitive causes [34]. In this study, GSE116918 data set was screened from the public GEO database and used for constructing a powerful nomogram to predict BCR in patients undergoing radical radiation therapy. We anticipated that the model will contribute to clinical decision-making and prognostic analysis.

A previous study by Yamamoto et al [35] showed that age at diagnosis, primary PSA level, baseline Gleason score, clinical T stage as well as number of high-risk factors were clinical factors

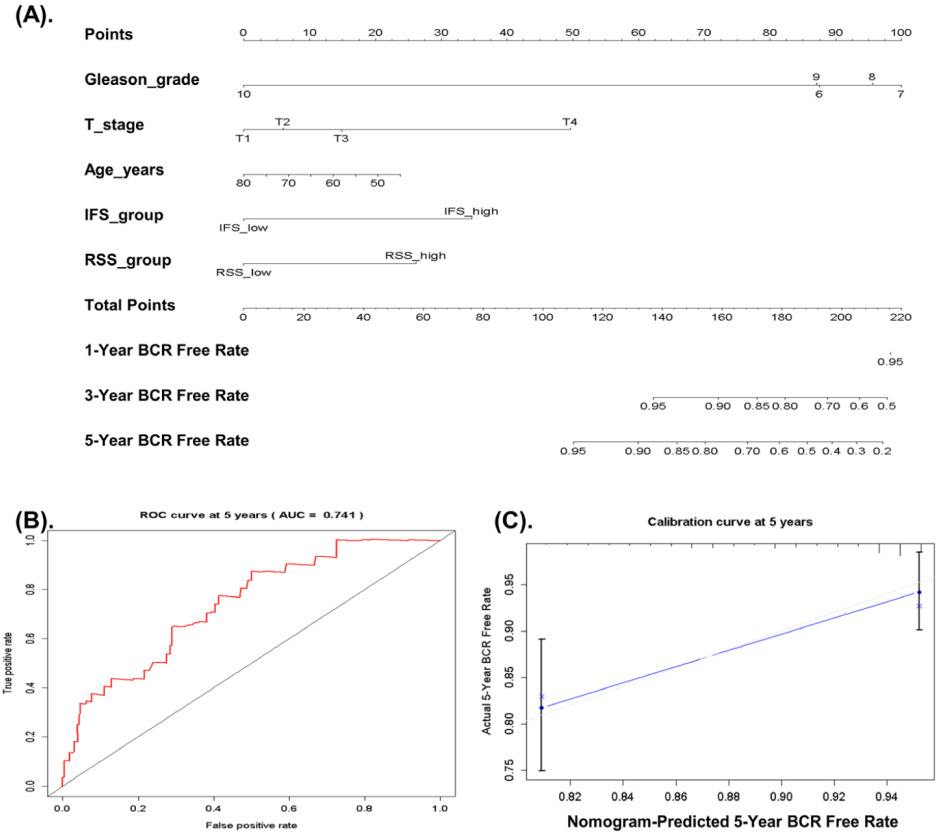

Figure 4. Development and evaluation of a prognostic nomogram. **A:** Construction of a prognostic nomogram. **B:** Receiver operating characteristic (ROC) curve of the nomogram. **C:** Calibration plot of the nomogram.

associated with BCR-free survival in patients with high-risk PCa treated with radiotherapy plus androgen deprivation therapy (ADT). However, few studies have taken cell radiosensitivity and immune infiltration into consideration as what we did in this study.

According to the result of survival analysis, the higher the IFS, the shorter the patient survival. With consideration of their coefficients in the formula of IFS, it was found that higher infiltration levels of macrophages, pDC, aDC, and NK_CD56bright were associated with higher IFS and worse prognosis while a higher expression level of neutrophils was associated with lower IFS and better prognosis, although only infiltration levels of macrophages, pDC, and aDC significantly differed among the three groups. A previous study [36] reported that macrophages promote circulating tumor cell-mediated local recurrence following radiotherapy in immunosuppressed patients, which is consistent with our results. However, to date, there is no research uncovering the association between primary existing dendritic cells, NK_CD56bright, and resistance to radiotherapy, therefore, more in-depth researches on the detailed mechanism are needed.

As shown in the results, the higher the RSS, the shorter the patient survival. With consideration of their coefficients in the formula of RSS, it was found that higher expression levels of BRCA2, BCL2L1, and MAPK13 were associated with higher RSS and worse prognosis, while higher expression levels of IGF1, MAPK1, and MAPK6 were associated with lower RSS and better prognosis, although only expression levels of IGF1 and BCL2L1 significantly differed among the three groups. A previous study has reported that BRCA status in breast tumors is related to sensitivity to radiation [37]. Osuka et al [38] found that IGF1 receptor signaling regulates adaptive radioprotection in glioma stem cells. MAP2K6 is also found to be associated with radiation resistance and adverse prognosis for locally advanced nasopharyngeal carcinoma patients [39]. However, there is no research concerning the relation of expression of other genes and radiotherapy, and it needs further research.

In this study, we constructed a visual nomogram to predict BCR after radical radiation therapy in PCa with fine discriminatory and calibration capacity, which took the elements, such as immune infiltration and radiosensitivity, into consideration for the first time. Although we have filled the gap to some extent, due to the lack of more effective clinical data, the predictive effect of this model cannot be effectively tested in an external database. In our future research work, we need to collect clinical materials from all aspects to validate the model. At the same time, we should further improve the prediction effect of the model so that would be more accurate and effective.

Acknowledgements

We thank LetPub (www.letpub.com) for its linguistic assistance during the preparation of this manuscript.

Author contribution

CQ designed the study and drafted the manuscript. XZ and HR were responsible for the collection and analysis of the experimental data. XZ, HR and ZC revised the manuscript critically for important intellectual content. All authors read and approved the final manuscript.

Conflict of interests

The authors declare no conflict of interests.

References

1. Rawla P. Epidemiology of Prostate Cancer. World J Oncol 2019;10:63-89.
2. Bolla M, Henry A, Mason M, Wiegel T. The role of radiotherapy in localised and locally advanced prostate cancer. Asian J Urol 2019;6:153-61.
3. Calleris G, Marra G, Dalmasso E et al. Is it worth to perform salvage radical prostatectomy for radio-recurrent prostate cancer? A literature review. World J Urol 2019;37:1469-83.
4. Zanatta DA, Andrade RJ, Pacagnan EF et al. Early stage prostate cancer: biochemical recurrence after treatment. Int Braz J Urol 2014;40:137-45.
5. Liu PH, Shah RB, Li Y et al. An IRAK1-PIN1 signalling axis drives intrinsic tumour resistance to radiation therapy. Nat Cell Biol 2019;21:203-13.
6. Aleksandrova E, Vlaykova T, Ananiev J, Gulubova M. Association of IL-12Bpro polymorphism with tumor-infiltrating dendritic cells in colorectal cancer. JBUON 2017;22:888-93.
7. Jain S, Lyons CA, Walker SM et al. Validation of a Metastatic Assay using biopsies to improve risk stratification in patients with prostate cancer treated with radical radiation therapy. Ann Oncol 2018;29:215-22.
8. Subramanian A, Tamayo P, Mootha VK, Mukherjee

S, Ebert BL, Gillette MA et al. Gene set enrichment analysis: a knowledge-based approach for interpreting genome-wide expression profiles. Proc Natl Acad Sci U S A 2005;102:15545-50.

9. Bindea G, Mlecnik B, Tosolini M et al. Spatiotemporal dynamics of intratumoral immune cells reveal the immune landscape in human cancer. Immunity 2013;39:782-95.
10. Newman AM, Liu CL, Green MR et al. Robust enumeration of cell subsets from tissue expression profiles. Nat Methods 2015;12:453-7.
11. Barbie DA, Tamayo P, Boehm JS et al. Systematic RNA interference reveals that oncogenic KRAS-driven cancers require TBK1. Nature 2009;462:108-12.
12. Hanzelmann S, Castelo R, Guinney J. GSVA: gene set variation analysis for microarray and RNA-seq data. BMC Bioinformatics 2013;14:7.
13. Rosen EM, Fan S, Goldberg ID, Rockwell S. Biological basis of radiation sensitivity. Part 2: Cellular and molecular determinants of radiosensitivity. Oncology (Williston Park) 2000;14:741-57.
14. Luo Y, Li M, Zuo X et al. betacatenin nuclear translocation induced by HIF1alpha overexpression leads to the radioresistance of prostate cancer. Int J Oncol 2018;52:1827-40.
15. Sims AH, Finnon P, Miller CJ et al. TPD52 and NFKB1 gene expression levels correlate with G2 chromosomal radiosensitivity in lymphocytes of women with and at risk of hereditary breast cancer. Int J Radiat Oncol Biol Phys 2007;83:409-20.
16. Aravindan S, Natarajan M, Herman TS, Awasthi V, Aravindan N. Molecular basis of 'hypoxic' breast cancer cell radio-sensitization: phytochemicals converge on radiation induced Rel signaling. Radiat Oncol 2013;8:46.
17. Sun D, Mu Y, Piao H. MicroRNA-153-3p enhances cell radiosensitivity by targeting BCL2 in human glioma. Biol Res 2018;51:56.
18. He J, Feng X, Hua J et al. miR-300 regulates cellular radiosensitivity through targeting p53 and apaf1 in human lung cancer cells. Cell Cycle 2017;16:1943-53.
19. Santos N, Silva RF, Pinto M et al. Active caspase-3 expression levels as bioindicator of individual radiosensitivity. An Acad Bras Cienc 2017;89:649-59.
20. Gurley KE, Ashley AK, Moser RD, Kemp CJ. Synergy between Prkdc and Trp53 regulates stem cell proliferation and GI-ARS after irradiation. Cell Death Differ 2017;24:1853-60.
21. Ahmed M, Li L, Pinnix C et al. ATM mutation and radiosensitivity: An opportunity in the therapy of mantle cell lymphoma. Crit Rev Oncol Hematol 2016;107:14-9.
22. Hosseini F, Sam MR, Jabbari N, Mozdarani H. Modulating Survivin as a Radioresistant Factor, Caspase-3, and Apoptosis by Omega-3 Docosahexaenoic Acid Sensitizes Mutant-p53 Colorectal Cancer Cells to gamma-Irradiation. Cancer Biother Radiopharm 2018;33:387-95.
23. Kan C, Zhang J. BRCA1 Mutation. A Predictive Marker for Radiation Therapy? Int J Radiat Oncol Biol Phys 2015;93:281-93.
24. Baert A, Depuydt J, Van Maerken T et al. Analysis of chromosomal radiosensitivity of healthy BRCA2 mutation carriers and non-carriers in BRCA families with the G2 micronucleus assay. Oncol Rep 2017;37:1379-86.
25. Wang M, Han J, Marcar L et al. Radiation Resistance in KRAS-Mutated Lung Cancer Is Enabled by Stem-like Properties Mediated by an Osteopontin-EGFR Pathway. Cancer Res 2017;77:2018-28.
26. Pomp J, Ouwerkerk IJ, Hermans J et al. The influence of the oncogenes NRAS and MYC on the radiation sensitivity of cells of a human melanoma cell line. Radiat Res 1996;146:374-81.
27. Jones HA, Hahn SM, Bernhard E, McKenna WG. Ras inhibitors and radiation therapy. Semin Radiat Oncol 2001;11:328-37.
28. Warenius HM, Jones M, Gorman T et al. Combined RAF1 protein expression and p53 mutational status provides a strong predictor of cellular radiosensitivity. Br J Cancer 2000;83:1084-95.
29. Hossain MB, Shifat R, Johnson DG et al. TIE2-mediated tyrosine phosphorylation of H4 regulates DNA damage response by recruiting ABL1. Sci Adv 2016;2:e1501290.
30. Wang T, Dong XM, Zhang FL, Zhang JR. miR-206 enhances nasopharyngeal carcinoma radiosensitivity by targeting IGF1 . Kaohsiung J Med Sci 2017;33:427-32.
31. Loriot Y, Mordant P, Dugue D et al. Radiosensitization by a novel Bcl-2 and Bcl-XL inhibitor S44563 in small-cell lung cancer. Cell Death Dis 2014;5:e1423.
32. Wang B, Ge Y, Gu X. Analysis of esophageal cancer cell lines exposed to X-ray based on radiosensitivity influence by tumor necrosis factor-alpha. J Xray Sci Technol 2016;24:761-9.
33. Eder S, Arndt A, Lamkowski A et al. Baseline MAPK signaling activity confers intrinsic radioresistance to KRAS-mutant colorectal carcinoma cells by rapid up-regulation of heterogeneous nuclear ribonucleoprotein K (hnRNP K). Cancer Lett 2017;385:160-7.
34. Zhang Y, Zhang J, Liang S, Lang G, Liu G, Liu P, Deng X.. Long non-coding RNA VIM-AS1 promotes prostate cancer growth and invasion by regulating epithelial-mesenchymal transition JBUON 2019;24:2090-8.
35. Yamamoto Y, Kiba K, Yoshikawa M, Hirayama A, Kunikata S, Uemura H. Evaluation of biochemical recurrence in patients with high-risk prostate cancer treated with radical prostatectomy and radiotherapy plus androgen deprivation therapy. Res Rep Urol 2016;8:225-31.
36. Rafar M, Aguilera TA, Vilalta M et al. Macrophages promote circulation tumor cell-mediated local recurrence following radiotherapy in immunosuppressed patients. Cancer Res 2018;78:4241-52.
37. Kirova YM, Stoppa-Lyonnet D, Savignoni A et al. Risk of breast cancer recurrence and contralateral breast cancer in relation to BRCA1 and BRCA2 mutation status following breast-conserving surgery and radiotherapy. Eur J Cancer 2005;41:2304-11.
38. Osuka S, Sampetrean O, Shimizu T et al. IGF1 receptor signaling regulates adaptive radioprotection in glioma stem cells. Stem Cells 2013;31:627-40.
39. Li Z, Li N, Shen L. MAP2K6 is associated with radiation resistance and adverse prognosis for locally advanced nasopharyngeal carcinoma patients. Cancer Manag Res 2018;10:6905-12.

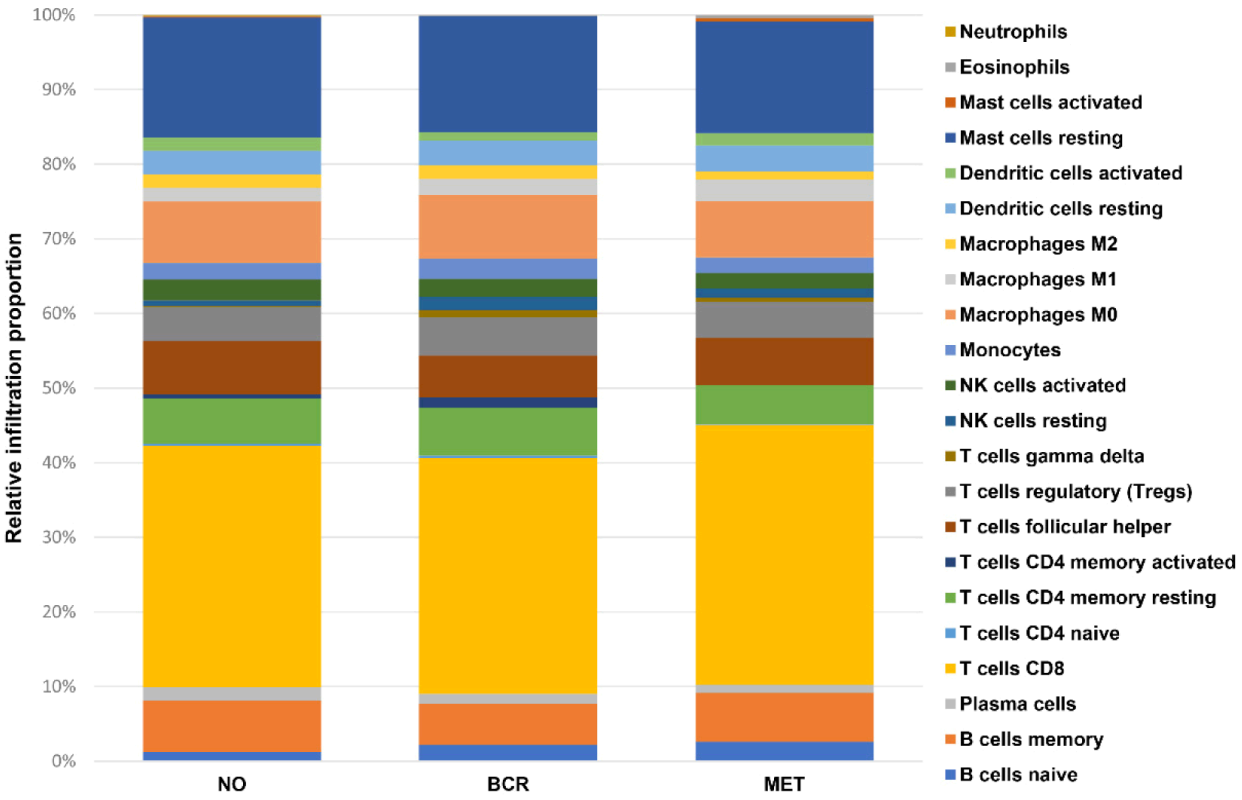

Suppl Figure 1. The mean relative fractions of 22 kinds of immune cells in NO, BCR and MET group by CIBERSORT.

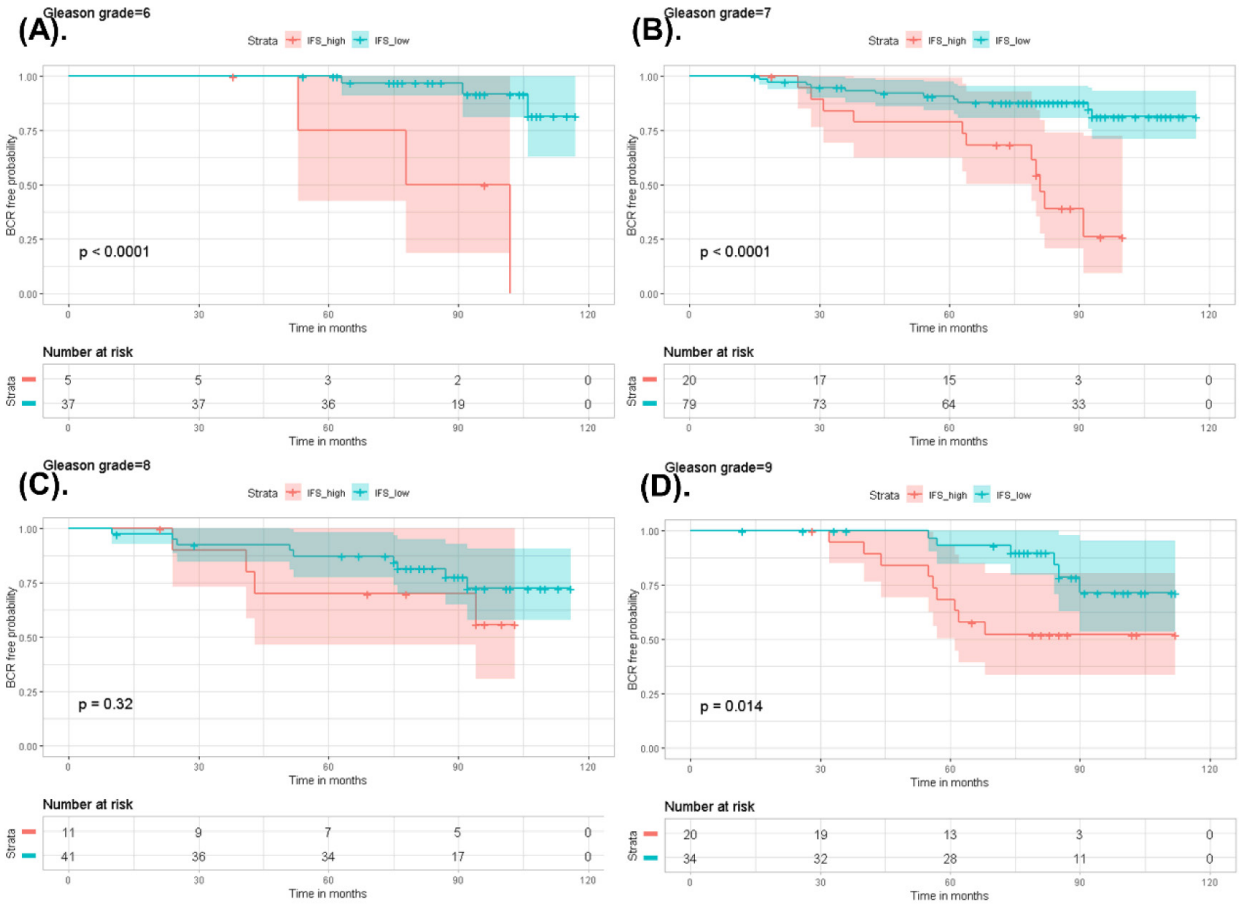

Suppl Figure 2. K-M plot of BCR-free survival of IFS groups adjusted by Gleason grade.

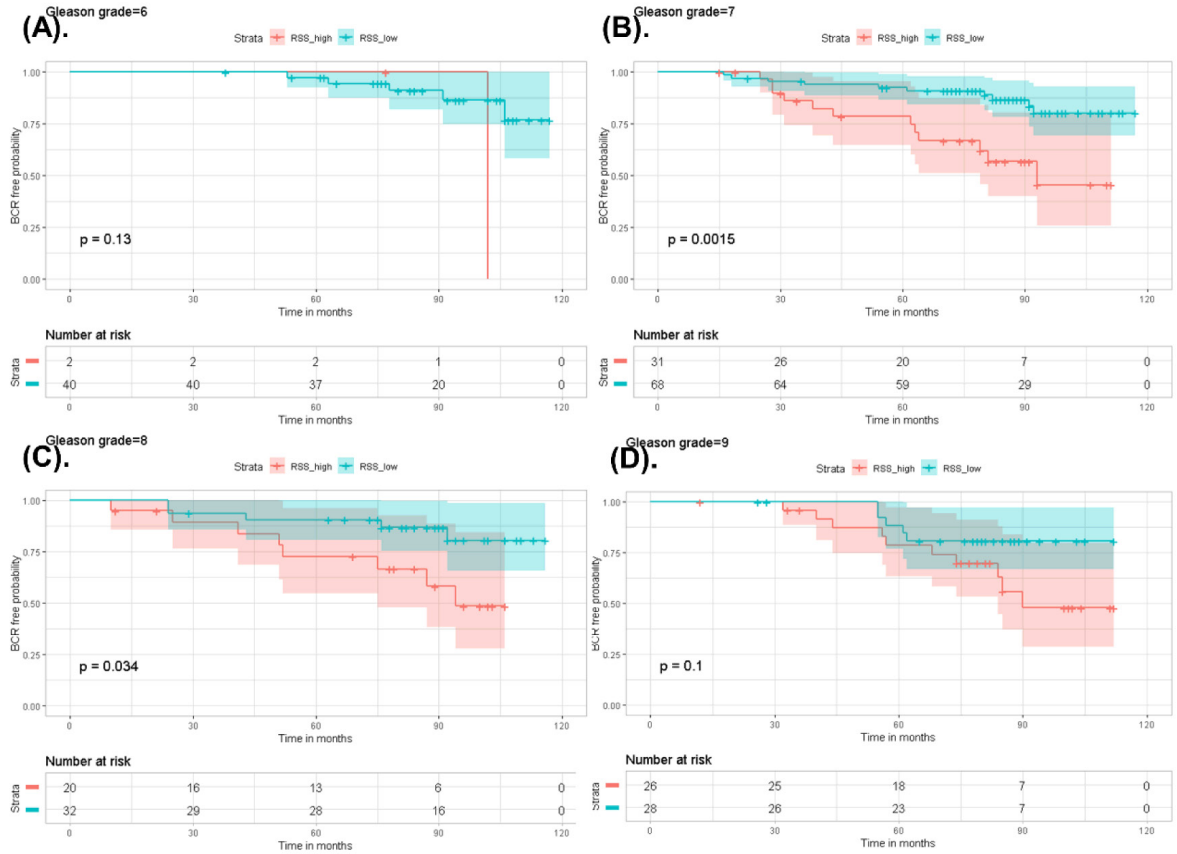

Suppl Figure 3. K-M plot of BCR-free survival of RSS groups adjusted by Gleason grade.

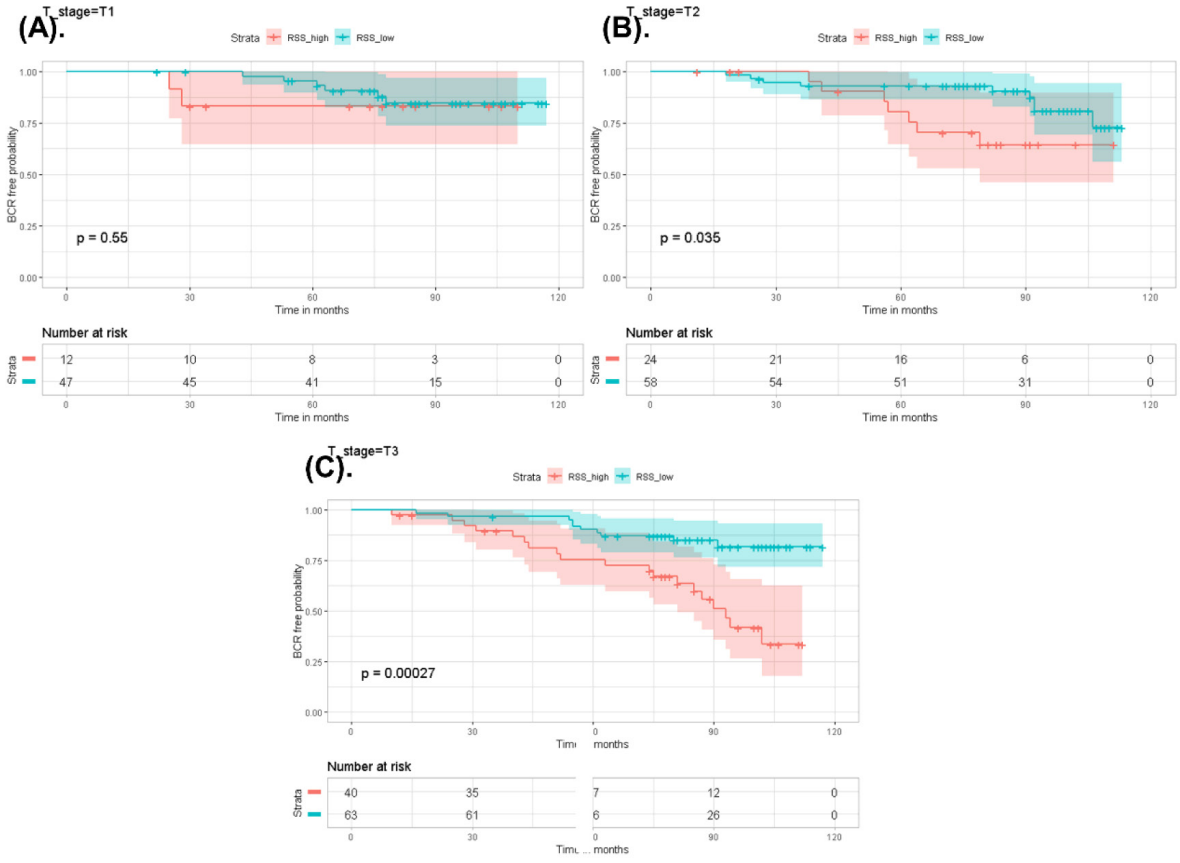

Suppl Figure 4. K-M plot of BCR-free survival of RSS groups adjusted by T stage.